IOWA STATE UNIVERSITY
Digital Repository

1969

A modal solution of the microstrip transmission line

Lawrence Griffith Heller
Iowa State University

Follow this and additional works at: https://lib.dr.iastate.edu/rtd

Part of the Electrical and Electronics Commons

Recommended Citation

70-13,590

HELLER, Lawrence Griffith, 1938-
A MODAL SOLUTION OF THE MICROSTRIP TRANS-
MISSION LINE.

Iowa State University, Ph.D., 1969
Engineering, electrical

University Microfilms, Inc., Ann Arbor, Michigan

A MODAL SOLUTION OF THE MICROSTRIP TRANSMISSION LINE

by

Lawrence Griffith Heller

A Dissertation Submitted to the

Graduate Faculty in Partial Fulfillment of

The Requirements for the Degree of

DOCTOR OF PHILOSOPHY

Major Subject: Electrical Engineering

Approved:

In Charge of Major Work

Head of Major Department

Dean of Graduate College

Iowa State University
Ames, Iowa

1969

PLEASE NOTE:

Not original copy.
Some pages have very
light type. Filmed
as received.

University Microfilms

TABLE OF CONTENTS

I. INTRODUCTION

In the years since 1945 there has been much interest in electro-
magnetic-wave transmission lines formed of various configurations of strip
conductors. A general cross-sectional view of a strip conductor trans-
mission line is shown in Figure 1. If $\epsilon_1 \neq \epsilon_2$, the configuration is called
a microstrip line. To eliminate confusion, it is sometimes necessary to
distinguish between the case when $b = \infty$ and when b is finite. This
distinction is made by using the terms open microstrip and shielded
microstrip. When $\epsilon_1 = \epsilon_2$, the transmission line is called a stripline.
The shielded microstrip line reduces to the stripline as either $a \rightarrow 0$
or $\epsilon_1 \rightarrow \epsilon_2$.

Because of its simplicity of fabrication, the microstrip-type
transmission line is becoming increasingly popular in both the microwave
community and the computer industry. Most known analytical solutions for
the microstrip line assume that the mode of propagation resembles the TEM
or transmission line mode. The TEM mode assumption reduces the analysis
of the microstrip line to a two-dimensional electrostatic fields problem
in the x-z plane. The electrostatic problem has been solved by methods
such as conformal mapping (1), image theory (2), the relaxation method
(3), and the variational principle (4). Although the TEM mode cannot
exist on the microstrip line (5, 6), the results of such an analysis to
determine the transmission line parameters agree well with experimental
measurements at low frequencies. At microwave frequencies, properties of
the actual microstrip mode such as dispersion and excitation of surface
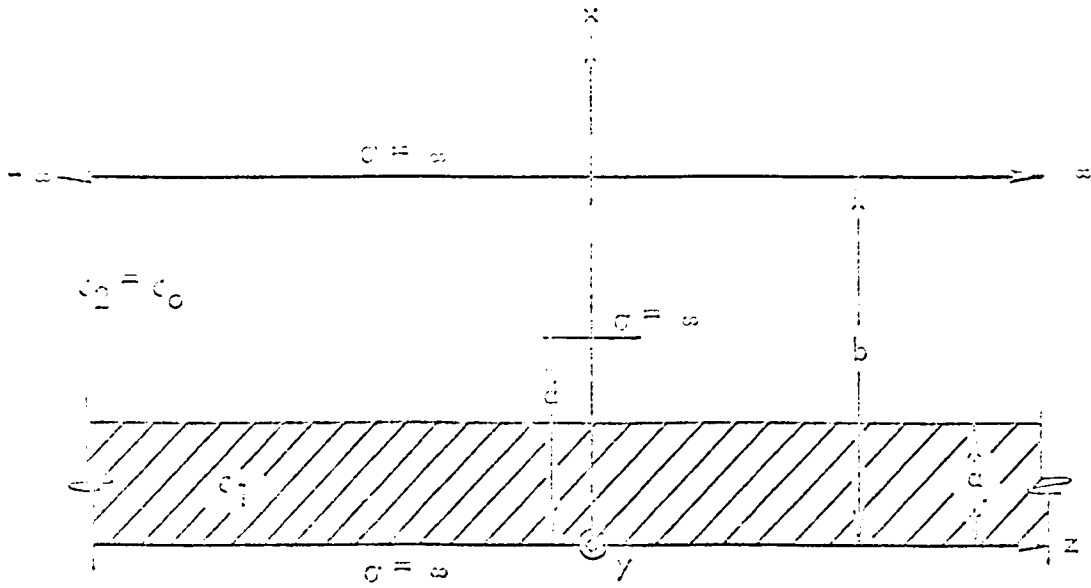waves cannot be explained by a TEM mode analysis. Recently, the dispersive

Figure 1. Strip conductor transmission line

characteristics of the open microstrip and shielded microstrip lines have
been studied in detail by Denlinger (7) and by Zysman and Varon (6),
respectively. These studies do not assume the TEM mode. Denlinger
solved an integral equation numerically for the propagation constant,
$k_y(\omega)$, of the microstrip line. A pair of coupled homogeneous Fredholm
integral equations of the first kind are solved numerically for $k_y(\omega)$
by Zysman and Varon.

Although the field analysis of the actual microstrip mode has been
considered (6, 7, 8), there seems to be very little useful information
available in the form of an accessible formula for the electromagnetic
fields of the microstrip line. The question of whether the actual fields
of the microstrip resemble the TEM mode has not been answered.

The open microstrip transmission line is known to excite surface
waves (9, 10). However, there seems to be doubt as to just which surface
wave modes are excited. The microstrip line is a traveling wave source
since the propagation constant, $k_y(\omega)$, is much greater than zero. This
means that the separation equations of the familiar two-dimensional surface
wave modes must be changed to include the effect of propagation in the y
direction. The propagation properties of the surface waves associated
with the microstrip line are not clearly understood.

The form of the longitudinal component of current, I_y, on the micro-
strip is known (7, 11). Unless the microstrip is formed of insulated
parallel filaments, there must be a transverse z-directed component of
current (6). However, it is expected that the transverse component of
current does not seriously affect the microstrip fields (7). The effect
of assuming $I_z = 0$ will be considered later.

II. STATEMENT OF PROBLEM

The purpose of this work is to attempt to fill in some of the missing field theory of the microstrip transmission line. Since the longitudinal component of current on the microstrip is known and the transverse current can usually be neglected, it is sufficient to determine the two-dimensional Green's function for the microstrip. The Green's function used here describes the fields due to a traveling wave line source in free space of phasor current density given by $\vec{J} = \vec{a}_y \delta(z)\delta(x - d)e^{-jk_y y}$. The microstrip propagation constant, k_y, will be considered known (7, 8). It is valid to place the traveling wave source in free space rather than on an actual conductor because the fields radiated will be the same in either case, provided the current density is correct (12).

The fields of the shielded microstrip will be found in terms of the complete set of source-free normal modes of the boundary value problem. The open microstrip is a singular Sturm-Liouville boundary value problem in the x direction. As such, the total fields must be expanded in a discrete surface wave spectrum plus a continuous spectrum. The continuous spectrum part of the fields can be found, with much numerical work, by integral transform methods (6, 7). Since the analysis used in this work does not seem to shed much light on the continuous spectrum, only the surface wave spectrum for the open microstrip will be considered in detail. The discrete spectrum of the open microstrip is very important in its own right because it changes radically with frequency.

The Green's function for the stripline is found essentially for the purpose of checking the results that are found for the microstrip line.

The scripline fields will be shown to be transverse magnetic to y (TM_y). For the case when $k_y = k_o = \omega\sqrt{\mu_o \epsilon_o}$, the TM_y solution will reduce to the known TEM mode solution.

Throughout this work, block letters will indicate phasor quantities. Although there will be no cause to convert the phasors over to the real time fields, the usual notation for real time fields is a script letter. The two notations are related by, for example, $\overline{\mathcal{E}}(x,y,z,t) = Re\overline{E}(x,y,z)e^{j\omega t}$. The units to be used are the rationalized MKSC system of units.

III. GREEN'S FUNCTION FOR THE STRIPLINE

We want to find the fields in the stripline configuration shown in Figure 1. The problem can be formulated in free space in terms of an infinite number of images of the actual source. The images of the actual source are on the x-axis and point in the + or - y direction. In free space, the vector potential, $\overline{A}$, is oriented in the same direction as the current, so $\overline{A} = A\overline{u}_y$. Since $\overline{B} = \overline{\nabla} \times \overline{A}$, $B_y = 0$ and the fields must be TM_y.

The fields between the two perfectly-conducting plates can be found in terms of a sum of TM_z plus TE_z, TM_x plus TE_x, or TM_y plus TE_y source-free normal modes because these three sets of modes each form a complete set (13). Since the TE_y modes are not excited by the assumed source, the TM_y formulation of the problem is the easiest.

The procedure is to sum the TM_y modes that propagate in the + and - z direction. The sum will include cutoff modes. From Harrington (14), the TM_y fields are related to a wave function ψ by

$$E_y = \frac{1}{j\omega\varepsilon_o}(\frac{\partial^2}{\partial y^2} + k_o^2)\psi \qquad H_y = 0$$

$$E_z = \frac{1}{j\omega\varepsilon_o}\frac{\partial^2\psi}{\partial y\partial z} \qquad H_z = \frac{\partial\psi}{\partial x} \qquad (1)$$

$$E_x = \frac{1}{j\omega\varepsilon_o}\frac{\partial^2\psi}{\partial y\partial x} \qquad H_x = -\frac{\partial\psi}{\partial z}$$

where $\psi \propto A_y$ and $k_o^2 = \omega^2\mu_o\varepsilon_o$. The boundary conditions that must be met at the conducting plate surfaces are $H_x = E_z = E_y = 0$. Suitable source-free mode wave functions for waves propagating in the + and - z direction are
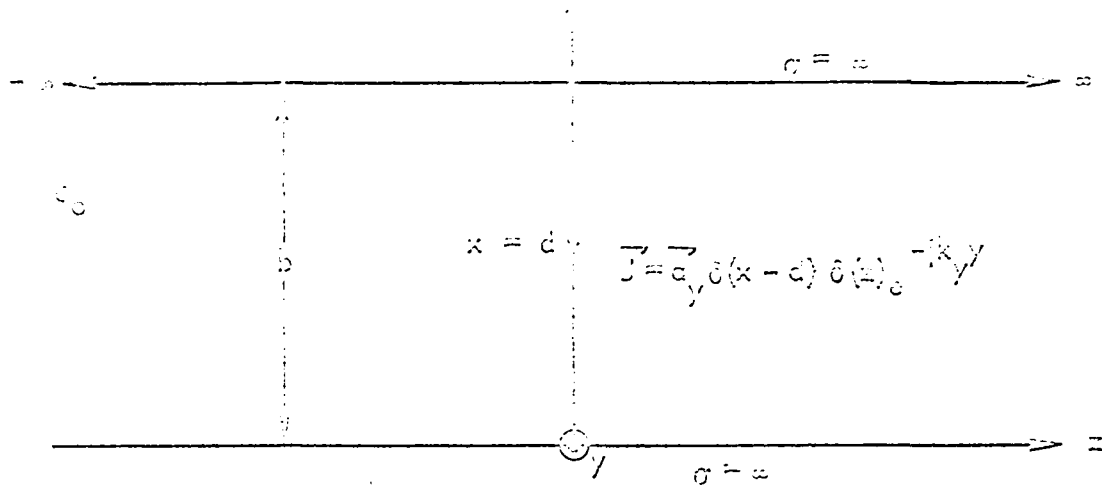
$$\sigma = \infty$$

$$\epsilon_0$$

$$b$$

$$x = d$$

$$\vec{J} = \vec{a}_y \, \delta(x - d) \, \delta(z) e^{-jky}$$

$$\sigma = \infty$$

Figure 2. The stripline

$$\psi_n^{\pm} = F_n^{\pm} \sin \frac{n\pi}{b} x \, e^{-jk_y y} \, e^{-\gamma_n |z|} \tag{2}$$

for n = 1,2,3, ···. ψ_n is a solution of the Helmholtz equation, $\nabla^2 \psi_n + k_0^2 \psi_n = 0$, so the separation equation is

$$\left(\frac{n\pi}{b}\right)^2 + k_y^2 - \gamma_n^2 = k_0^2 \tag{3}$$

The procedure of expanding ψ in terms of ψ_n is outlined by Harrington (14). Let

$$\psi^{\pm} = \sum_{n=1}^{\infty} \psi_n^{\pm} \tag{4}$$

E_y must be continuous at z = 0. Using Equation 1, this requires that $F_n^+ = F_n^- = F_n$ or equivalently that $\psi^+ = \psi^- = \psi$. The source condition at z = 0 is

$$\delta(x - d)e^{-jk_y y} = [H_x^+ - H_x^-]_{z=0} \tag{5}$$

Using Equations 1, 2, 4, and 5, we have

$$\delta(x - d) = 2 \sum_{n=1}^{\infty} F_n \gamma_n \sin \frac{n\pi}{b} x \tag{6}$$

This equation can be multiplied by $\sin \frac{m\pi}{b} x$ and integrated term by term on x from x = 0 to x = b (15). This results in

$$F_n = \frac{\sin \frac{n\pi}{b} d}{\gamma_n b} \tag{7}$$

From Equation 4,

$$\psi = e^{-jk_y y} \sum_{n=1}^{\infty} \frac{\sin \frac{n\pi}{b} d \, \sin \frac{n\pi}{b} x}{\gamma_n b} e^{-\gamma_n |z|} \tag{8}$$

where $\gamma_n = \sqrt{(\frac{n\pi}{b})^2 + k_y^2 - k_o^2}$. The sign on this radical is chosen so that each term in the series of Equation 8 represents propagation or decay away from the source. The fields are found by substituting Equation 8 into Equation 1. Either ϕ or the fields found from Equation 1 can be called the Green's function for the stripline.

Setting $k_y = k_o$ in Equations 1 and 8 reduces the TM_y analysis above to the TEM_y stripline mode. The TEM_y mode should have the same transverse dependence as the fields of a static line charge at $z = 0$ and $x = d$ (13). That is, it should be possible to put $\overline{E}$ in the form

$$\overline{E} = - \overline{\nabla}_t \phi(x,z) e^{-jk_o y} \tag{9}$$

where $\phi(x,z)$ is the potential of a static line charge between two grounded plates and $\overline{\nabla}_t = \overline{a}_x \frac{\partial}{\partial x} + \overline{a}_z \frac{\partial}{\partial z}$.

From Equation 1,

$$\overline{E} = \frac{1}{j\omega\varepsilon_o}[\frac{\partial}{\partial x}(\frac{\partial \psi}{\partial y})\overline{a}_x + \frac{\partial}{\partial z}(\frac{\partial \psi}{\partial y})\overline{a}_z] = \frac{1}{j\omega\varepsilon_o}\overline{\nabla}_t(\frac{\partial \psi}{\partial y}) \tag{10}$$

Comparing Equations 9 and 10 yields

$$\phi(x,z) = \sqrt{\frac{\mu_o}{\varepsilon_o}} \sum_{n=1}^{\infty} \frac{\sin \frac{n\pi}{b} d \sin \frac{n\pi}{b} x}{n\pi} e^{-\frac{n\pi}{b}|z|} \tag{11}$$

Using the continuity equation gives the charge density as

$$\rho = - \frac{\overline{\nabla}\cdot\overline{J}}{j\omega} = \delta(x - d)\delta(z)/\mu_o\varepsilon_o \, e^{-jk_o y} \tag{12}$$

By letting $\omega \to o$, the static charge density is found to be

$$\rho = \delta(x - d)\delta(z)/\mu_o\varepsilon_o \tag{13}$$

The static Green's function, $G,$ is the potential due to a unit line

charge. Hence,

$$G(x,z) = \frac{1}{\sqrt{\mu_0 \epsilon_0}} \phi(x,z) = \frac{1}{\epsilon_0} \sum_{n=1}^{\infty} \frac{\sin \frac{n\pi}{b} d \sin \frac{n\pi}{b} x \, e^{-\frac{n\pi}{b}|z|}}{n\pi} \tag{14}$$

This Green's function compares exactly with that given by Kraut (16).

The results of the above TM_y mode analysis for the stripline Green's function will be used as a basis to check later results.

IV. GREEN'S FUNCTION FOR THE SHIELDED MICROSTRIP LINE

The shielded microstrip configuration to be analyzed is shown in Figure 3. The reason for putting a $\cos k_y y$ dependence in the current density will become evident later. An attempt to formulate a TM_y solution for the microstrip would ultimately prove fruitless, except in the special case when $k_y = 0$. When $\frac{\partial}{\partial y} \neq 0$, Sommerfeld (17) has shown that there cannot be a TM_y solution because the dielectric slab boundary conditions require a component of $\bar{A}$ to be transverse to the microstrip. By assuming a component of $\bar{J}$ in the z direction, the source problem could probably be formally solved by a Fourier transform analysis (6). However, the method of solution in this work will be to sum the source-free normal TE_x and TM_x modes.

Before beginning the analysis, some of the theory of uniform waveguides must be presented. The theory outlined below is covered in detail by Collin (13). With the assumed $\cos k_y y$ dependence in $\bar{J}$, it will later be shown that perfectly conducting walls in the $y = \pm m\pi/k_y$ planes, $m = 1,2,3 \cdots$, can be placed along the microstrip line without having any effect on the fields. In fact, the field analysis will reduce to considering an inhomogeneously filled rectangular waveguide shown in Figure 4. The normal modes of the dielectric slab loaded guide are confined to only TE_x and TM_x modes. However, an arbitrary field in the slab guide can be represented as an infinite series over the normal modes (13). The notation for the nth normal mode fields will be
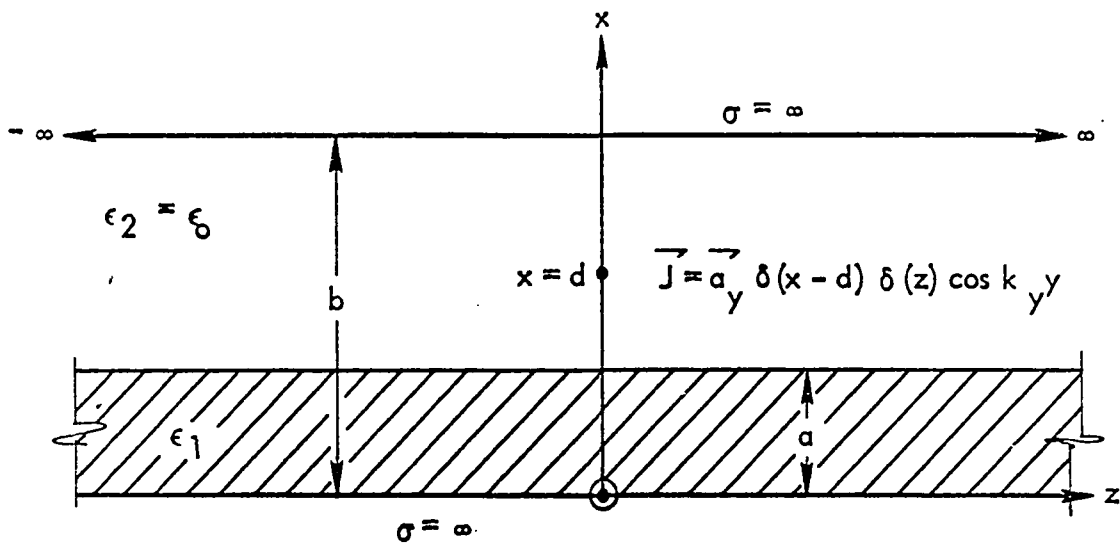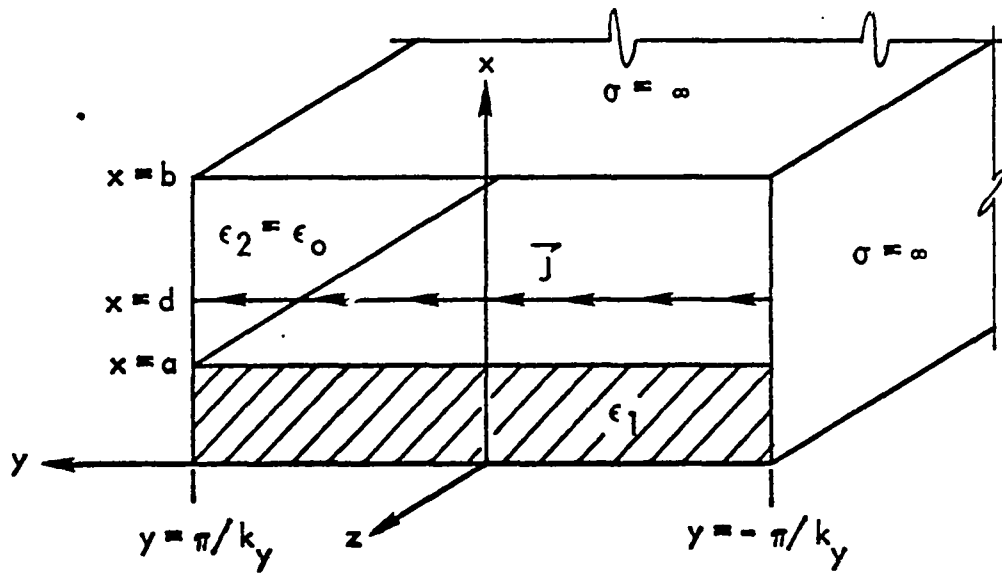
Figure 3.   The shielded microstrip

Figure 4. Inhomogeneously filled waveguide

$$\overrightarrow{E}{}^{\pm}_n = (\overrightarrow{e}_n \pm \overrightarrow{e}_{zn})e^{\mp \Gamma_n z}$$

$$\overrightarrow{H}{}^{\pm}_n = (\pm \overrightarrow{h}_n + \overrightarrow{h}_{zn})e^{\mp \Gamma_n z}$$

(15)

where

$$\overrightarrow{e}_n = \overrightarrow{e}_n(x,y) = \text{the modal transverse electric field} \qquad (16)$$

$$\overrightarrow{h}_n = \overrightarrow{h}_n(x,y) = \text{the modal transverse magnetic field} \qquad (17)$$

$$\overrightarrow{e}_{zn} = \overrightarrow{e}_{zn}(x,y) = \text{the modal axial electric field} \qquad (18)$$

$$\overrightarrow{h}_{zn} = \overrightarrow{h}_{zn}(x,y) = \text{the modal axial magnetic field} \qquad (19)$$

In Equation 15, it is assumed that the normal mode fields are normalized such that

$$\iint_S \overrightarrow{e}_n \times \overrightarrow{h}_n \cdot \overrightarrow{a}_z da = \int_{-y_1}^{y_1} \int_0^b \overrightarrow{e}_n \times \overrightarrow{h}_n \cdot \overrightarrow{a}_z dx\ dy = 1 \qquad (20)$$

where $y_1 = \pi/k_y$. The modes are orthogonal in the sense that

$$\iint_S \overrightarrow{e}_n \times \overrightarrow{h}_m \cdot \overrightarrow{a}_z da = 0 \qquad n \neq m \qquad (21)$$

If one mode in Equation 21 is TE_x and one is TM_x, then Equation 21 holds when $n = m$. The fields radiated in the + and − z direction by the micro-strip are represented as

$$\overrightarrow{E}{}^{\pm} = \sum_n a_n \overrightarrow{E}{}^{\pm}_n$$

$$\overrightarrow{H}{}^{\pm} = \sum_n a_n \overrightarrow{H}{}^{\pm}_n$$

(22)

where the sum is over both the TE_x and TM_x normal modes. The coefficients, a_n, are found by Collin (13) through an application of the Lorentz reciprocity principle as

$$a_n = -\frac{1}{2} \int_V \vec{J} \cdot \vec{E}_n^+ \, dv = -\frac{1}{2} \int_{-1}^{1} \int_{-y_1}^{y_1} \int_0^b \vec{J} \cdot \vec{E}_n^+ \, dxdydz \qquad (23)$$

The conducting walls at $y = \pm \pi/k_y$ are needed in the derivation of

Equation 23. To eliminate some confusion, the microstrip fields will be

partitioned into a TE_x part and a TM_x part. All this means is that the

sums in Equation 22 will be found in two parts. The total field is the

sum of the TE_x part and the TM_x part.

A. TE_x Fields

The TE_x fields are related to a wave function ψ_h by

$$E_{xh} = 0 \qquad\qquad H_{xh} = \frac{1}{j\omega\mu_o}\left(\frac{\partial^2}{\partial x^2} + k^2\right)\psi_h$$

$$E_{yh} = -\frac{\partial \psi_h}{\partial z} \qquad\qquad H_{yh} = \frac{1}{j\omega\mu_o}\frac{\partial^2 \psi_h}{\partial x \partial y} \qquad (24)$$

$$E_{zh} = \frac{\partial \psi_h}{\partial y} \qquad\qquad H_{zh} = \frac{1}{j\omega\mu_o}\frac{\partial^2 \psi_h}{\partial x \partial z}$$

where the subscript h is used to indicate TE_x fields and $k^2 = \omega^2\mu_o\epsilon(x)$.

The wave function for the nth mode must be chosen so that the fields meet

the correct boundary conditions at the dielectric interface and on the

conductor surface. The required boundary conditions are continuity of

E_y, E_z, H_y, and H_z at $x = a$ and $\vec{E}_{tangential} = 0$ on the conductor surfaces.

The suitable wave function for the $\pm$ wave is (14)

$$\psi_{hn}^{\pm} = c_n e^{\mp \Gamma_n z}\left\{\frac{\sin t_n L}{\sin f_n a} \sin f_n x[1-u(x-a)]+\sin t_n(b-x)u(x-a)\right\}\cos k_y y$$

$$(25)$$

where

$$u(x - a) = \begin{cases} 1, & x > a \\ 0, & x < a \end{cases} \tag{26}$$

$$f_n^2 + k_y^2 - \Gamma_n^2 = k_1^2 = \omega^2 \epsilon_1 \mu_o \tag{27}$$

$$t_n^2 + k_y^2 - \Gamma_n^2 = k_o^2 = \omega^2 \epsilon_o \mu_o \tag{28}$$

$$f_n \cot f_n a = - t_n \cot t_n L \tag{29}$$

$$L = b - a \tag{30}$$

The meaning of u(x-a), in this work, is symbolic in the sense that

derivatives of functions involving u(x-a) will not be taken at x = a. The

boundary conditions at x = a will automatically be met by this procedure.

We need consider only the + wave in the following analysis; omitting

the ± superscript should not cause any confusion. Putting Equation 25

into Equation 24 gives the TE_x modal fields as

$$E_{xhn} = 0 \tag{31}$$

$$E_{yhn} = \Gamma_n \psi_{hn} \tag{32}$$

$$E_{zhn} = - k_y \tan k_y y \, \psi_{hn} \tag{33}$$

$$H_{xhn} = \frac{1}{j\omega\mu_o} (k_y^2 - \Gamma_n^2) \psi_{hn} \tag{34}$$

$$H_{yhn} = - \frac{C_n k_y \sin k_y y}{j\omega\mu_o} \{ \frac{\sin t_n L}{\sin f_n a} f_n \cos f_n x [1-u(x-a)]$$
$$- t_n \cos t_n (b-x) u(x-a) \} e^{-\Gamma_n z} \tag{35}$$

$$H_{zhn} = - \frac{\Gamma_n C_n}{j\omega\mu_o} \{ \frac{\sin t_n L}{\sin f_n a} f_n \cos f_n x [1-u(x-a)]$$
$$- t_n \cos t_n (b-x) u(x-a) \} \cos k_y y \, e^{-\Gamma_n z} \tag{36}$$

Note that E_{zhn} and H_{yhn} are zero at $y = \pm \pi/k_y$. From Equations 31, 32, 34, 35, and 15, we have

$$\vec{e}_{hn} = \Gamma_n e^{+\Gamma_n z} \psi_{hn} \vec{a}_y \qquad (37)$$

$$\vec{h}_{hn} = \frac{1}{j\omega\mu_o} (k_y^2 - \Gamma_n^2) \psi_{hn} e^{+\Gamma_n z} \vec{a}_x$$

$$- \frac{C_n k_y \sin k_y y}{j\omega\mu_o} \{\frac{\sin t_n L}{\sin f_n a} f_n \cos f_n x [1-u(x-a)] - t_n \cos t_n (b-x) u(x-a)\} \vec{a}_y \qquad (38)$$

For Equation 20 to be valid, C_n is chosen so that

$$\iint_S \vec{e}_{hn} \times \vec{h}_{nm} \cdot \vec{a}_z \, da = \delta_{nm} = \begin{cases} 1, & n=m \\ 0, & n \neq m \end{cases} \qquad (39)$$

In Appendix A, the integration indicated in Equation 39 is performed and C_n^2 evaluated as

$$C_n^2 = \frac{-4j\omega\mu_o k_y t_n f_n}{\Gamma_n (k_y^2 - \Gamma_n^2) \pi \{\frac{\sin^2 t_n L}{\sin^2 f_n a} (2t_n f_n a - t_n \sin 2f_n a) + t_n f_n L - f_n \sin 2t_n L\}} \qquad (40)$$

Using Equation 23, we have

$$a_{hn} = -\frac{1}{2} \int_V \vec{J} \cdot \vec{E}_{hn}^+ dv = -\frac{1}{2} \int_{-y_1}^{y_1} \int_{-1}^{1} \int_0^b \delta(x-d)\delta(z) \cos k_y y \Gamma_n \psi_{hn} \, dx\, dy\, dz \qquad (41)$$

Integrating yields

$$a_{hn} = -\frac{\pi \Gamma_n C_n \sin t_n (b-d)}{2k_y} \qquad (42)$$

Now that a_{nn} has been evaluated, the TE_x portion of the microstrip fields can be found. The simplest field representation is in terms of

$\psi_h^{\pm}$. To find $\psi_h^{\pm}$, start with Equations 22.

$$H_{hx}^{\pm} = \sum_n a_{hn} H_{hnx}^{\pm} = \pm \sum_n a_{hn} \{\frac{1}{j\omega\mu_o}(\frac{\partial^2}{\partial x^2} + k^2)\psi_{hn}^{\pm} \tag{43}$$

where Equations 15 and 24 have been used. The solutions of Equations 27, 28, and 29 can be numbered from 1 to ∞ so that Equation 43 becomes

$$H_{hx}^{\pm} = \frac{\pm 1}{j\omega\mu_o} (\frac{\partial^2}{\partial x^2} + k^2) \sum_{n=1}^{\infty} a_{hn}\psi_{hn}^{\pm} \tag{44}$$

Comparing with Equation 24 yields

$$\psi_h^{\pm} = \pm \sum_{n=1}^{\infty} a_{hn} \psi_{hn}^{\pm} \tag{45}$$

From Equations 25, 40, and 42,

$$\psi_h^{\pm} = \pm 2j\omega\mu_o \cos k_y y \sum_{n=1}^{\infty}$$

$$\frac{t_n f_n \sin t_n(b-d)\{\frac{\sin t_n L}{\sin f_n a} \sin f_n x[1-u(x-a)]+\sin t_n(b-x)u(x-a)\}e^{\mp\Gamma_n z}}{(k_y^2 - \Gamma_n^2)\{\frac{\sin^2 t_n L}{\sin^2 f_n a}(2t_n f_n a - t_n \sin 2f_n a) + 2t_n f_n L - f_n \sin 2t_n L\}} \tag{46}$$

The TE_x part of the shielded microstrip fields is found by putting Equation 46 into Equations 24.

B. TM_x Fields

The TM_x fields are related to a wave function ψ_e by

$$E_{xe} = \frac{1}{j\omega\varepsilon}(\frac{\partial^2}{\partial x^2} + k^2)\psi_e \qquad\qquad H_{xe} = 0$$

$$E_{ye} = \frac{1}{j\omega\varepsilon}\frac{\partial^2\psi_e}{\partial x\partial y} \qquad\qquad H_{ye} = \frac{\partial\psi_e}{\partial z} \qquad (47)$$

$$E_{ze} = \frac{1}{j\omega\varepsilon}\frac{\partial^2\psi_e}{\partial x\partial z} \qquad\qquad H_{ze} = -\frac{\partial\psi_e}{\partial y}$$

where the subscript e indicates TM_x fields and $k^2 = \omega^2\mu_o\varepsilon$ with $\varepsilon = \varepsilon(x)$.

The procedure here will parallel the TE_x field analysis of section IV-A.

The modal wave function that meets the required boundary conditions is

$$\psi_{en}^{\pm} = D_n\{\frac{\cos q_n L}{\cos p_n a}\cos p_n x[1-u(x-a)]+\cos q_n(b-x)u(x-a)\}\sin k_y y e^{\mp\gamma_n z} \qquad (48)$$

where

$$p_n^2 + k_y^2 - \gamma_n^2 = k_1^2 = \omega^2\varepsilon_1\mu_o \qquad (49)$$

$$q_n^2 + k_y^2 - \gamma_n^2 = k_o^2 = \omega^2\varepsilon_o\mu_o \qquad (50)$$

$$\frac{p_n}{\varepsilon_1}\tan p_n a = -\frac{q_n}{\varepsilon_o}\tan q_n L \qquad (51)$$

In the analysis below, the absence of a $\pm$ superscript indicates the +

wave. The TM_x modal fields are

$$E_{xen} = \frac{1}{j\omega\varepsilon}(k_y^2 - \gamma_n^2)\psi_{en} \qquad (52)$$

$$E_{yen} = \frac{D_n k_y \cos k_y y}{j\omega\varepsilon} \left\{ \frac{-\cos q_n L}{\cos p_n a} p_n \sin p_n x [1-u(x-a)] + q_n \sin q_n (b-x) u(x-a) \right\} e^{-\gamma_n z}$$

(53)

$$E_{zen} = \frac{-D_n \gamma_n}{j\omega\varepsilon} \left\{ \frac{-\cos q_n L}{\cos p_n a} p_n \sin p_n x [1-u(x-a)] + q_n \sin q_n (b-x) u(x-a) \right\} \sin k_y y \, e^{-\gamma_n z}$$

(54)

$$H_{xen} = 0 \tag{55}$$

$$H_{yen} = -\gamma_n \psi_{en} \tag{56}$$

$$H_{zen} = -k_y \cot k_y y \, \psi_{en} \tag{57}$$

Note that E_{xen}, E_{zen} and H_{yen} are zero at $y = \pm \pi/k_y$. Since E_{zhn} and H_{yhn} are also zero at $y = \pm \pi/k_y$, the original assumption of putting conductors at $y = \pm \pi/k_y$ is verified. From Equations 52, 53, 55, 56, and 15 we have

$$\vec{e}_{en} = \frac{1}{j\omega\varepsilon}(k_y^2 - \gamma_n^2) e^{\gamma_n z} \psi_{en} \vec{a}_x$$

$$+ \frac{D_n k_y \cos k_y y}{j\omega\varepsilon} \left\{ \frac{-\cos q_n L}{\cos p_n a} p_n \sin p_n x [1-u(x-a)] + q_n \sin q_n (b-x) u(x-a) \right\} \vec{a}_y$$

(58)

$$\vec{h}_{en} = -\gamma_n e^{\gamma_n z} \psi_{en} \vec{a}_y \tag{59}$$

D_n is chosen so that

$$\iint_S \vec{e}_{en} \times \vec{h}_{em} \cdot \vec{a}_z \, da = \delta_{nm} \tag{60}$$

The integration indicated in Equation 60 is carried out in Appendix A and D_n^2 evaluated as

$$D_n^2 = \frac{-4j\omega k_y p_n q_n \epsilon_o}{(k_y^2-\gamma_n^2)\gamma_n\pi\{\dfrac{\epsilon_o\cos^2 q_n L}{\epsilon_1\cos^2 p_n a}(2ap_n q_n+q_n\sin 2p_n a)+2q_n p_n L+p_n\sin 2q_n L\}} \tag{61}$$

From Equation 23,

$$a_{en} = -\frac{1}{2}\int_V \vec{J}\cdot\vec{E}_{en}^+\, dv$$

$$= -\frac{1}{2}\int_{-1}^{1}\int_{-y_1}^{y_1}\int_0^b \delta(x-d)\delta(z)\frac{k_y}{j\omega\epsilon}D_n q_n\cos^2 k_y y\sin q_n(b-d)e^{-\gamma_n z}dxdydz \tag{62}$$

Integrating yields,

$$a_{en} = -\frac{\pi D_n q_n\sin q_n(b-d)}{2j\omega\epsilon_o} \tag{63}$$

Proceeding as for the TE_x case, we have

$$E_{ex}^{\pm} = \sum_{n=0}^{\infty} a_{en}E_{enx}^{\pm} = \frac{1}{j\omega\epsilon}(\frac{\partial^2}{\partial x^2}+k^2)\sum_{n=0}^{\infty} a_{en}\psi_{en}^{\pm} \tag{64}$$

Comparing with Equation 47 yields

$$\psi_e^{\pm} = \sum_{n=0}^{\infty} a_{en}\psi_{en}^{\pm} \tag{65}$$

The sum starts with n = 0 so that there is a correspondence with the empty waveguide modes. Using Equations 48, 61, and 63 yields

$$\psi_e^{\pm} = 2k_y\sin k_y y\sum_{n=0}^{\infty}$$

$$\frac{p_n q_n^2\sin q_n(b-d)\{\dfrac{\cos q_n L}{\cos p_n a}\cos p_n x[1-u(x-a)]+\cos q_n(b-x)u(x-a)\}e^{+\gamma_n z}}{(k_y^2-\gamma_n^2)\gamma_n\{\dfrac{\epsilon_o\cos^2 q_n L}{\epsilon_1\cos^2 p_n a}(2ap_n q_n+q_n\sin 2p_n a)+2q_n p_n L+p_n\sin 2q_n L\}} \tag{66}$$

The TM_x part of the shielded microstrip fields is found by putting Equation 66 into Equations 47.

C. The Total Shielded Microstrip Fields

The total fields are the sum of the TM_x and TE_x fields. The procedure to get the shielded microstrip fields is to put Equations 46 and 66 into Equations 24 and 47, respectively, and add field components.

The microstrip fields found here do not include the effect of a transverse current on the microstrip. However, the analysis used in this work could handle a transverse microstrip current. The effect would be in the modal amplitudes and not in the normal mode propagation properties.

D. Some Checks of Results

In this section, the results for the shielded microstrip will be checked with the stripline results by two limiting processes. However, before going on, consider the microstrip line as $k_y \rightarrow 0$. This takes the y dependence out of $\vec{J}$ and the fields so that $\frac{\partial}{\partial y} = 0$. A glance at Equations 46, 66, and 24 shows that $\psi_e \rightarrow 0$ as $k_y \rightarrow 0$ and that the fields become both TE_x and TM_y. This justifies the former statement that a TM_y solution was only possible if $\frac{\partial}{\partial y} = 0$. The two-dimensional TM_y solution for the shielded microstrip can be readily solved by bilateral Laplace transform method. The result checks with the analysis given in section IV-A. Perhaps the most interesting aspect of the y independent Laplace transform solution of the shielded microstrip is that there are no branch points in the inversion integral. This is not the case when $b = \infty$ (13).

1. <u>The shielded microstrip as $a \to 0$</u>

As $a \to 0$, t_n and q_n must approach the corresponding empty guide

values given by Harrington (14). This results in

$$t_n \to \frac{n\pi}{L} \qquad n = 1,2,3, \cdots \tag{67}$$

$$q_n \to \frac{n\pi}{L} \qquad n = 0,1,2, \cdots \tag{68}$$

These results check with Equations 29 and 51. From Equations 29 and 67,

$$\frac{\sin t_n L}{\sin f_n a} = - \frac{t_n \cos t_n L}{f_n \cos f_n a} \tag{69}$$

and

$$\lim_{a \to 0} \frac{\sin^2 t_n L}{\sin^2 f_n a} = \frac{t_n^2}{f_n^2} \tag{70}$$

Also,

$$\sin \frac{n\pi}{L} (L-x) = (-1)^{n+1} \sin \frac{n\pi}{L} x \tag{71}$$

$$\cos \frac{n\pi}{L} (L-x) = (-1)^n \cos \frac{n\pi}{L} x \tag{72}$$

Putting the above equations into Equations 46 and 66 as $a \to 0$ yields

$$\psi_h^\pm \to \pm j\omega\mu_0 \cos k_y y \sum_{n=1}^{\infty} \frac{\sin \frac{n\pi}{L} d \sin \frac{n\pi}{L} x \; e^{\mp \Gamma_n z}}{(k_y^2 - \Gamma_n^2)L} \tag{73}$$

and

$$\psi_e^\pm \to - k_y \sin k_y y \sum_{n=1}^{\infty} \frac{(\frac{n\pi}{L}) \sin \frac{n\pi}{L} d \cos \frac{n\pi}{L} x \; e^{\mp \Gamma_n z}}{(k_y^2 - \Gamma_n^2) \Gamma_n L} \tag{74}$$

where

$$(\frac{n\pi}{L})^2 + k_y^2 - \Gamma_n^2 = k_o^2 \tag{75}$$

The $n = 0$ term is not included in Equation 74 because it is zero. An interesting aspect of the shielded microstrip line is that it excites the TM_{xo} mode while the stripline does not. The physical reason for this difference is that the TM_{xo} mode of the empty guide has $E_{yeo} = 0$ so that it does not react with $\vec{J}$. The TM_{xo} mode of the slab guide has a non-zero y component of electric field. The fields of the stripline are found from Equations 73 and 74 by putting them into Equations 24 and 47, respectively, and adding the field components. The results, for $\vec{J} = \vec{a}_y \delta(x-d)\delta(z)e^{-jk_y y}$, compares with the stripline fields of section III.

2. The shielded microstrip as $\epsilon_1 \rightarrow \epsilon_0$

Starting with Equations 27, 28, 49, and 50, it is seen that $p_n \rightarrow q_n$ and $f_n \rightarrow t_n$ as $\epsilon_1 \rightarrow \epsilon_0$. Equations 29 and 51 become

$$\cot t_n a = - \cot t_n(b - a) = \frac{\cot t_n b \cot t_n a + 1}{\cot t_n b - \cot t_n a} \tag{76}$$

and

$$\tan q_n a = - \tan q_n(b - a) = - \frac{\tan q_n b + \tan q_n a}{1 + \tan q_n b \tan q_n a} \tag{77}$$

The expected empty guide result is

$$q_n = p_n = t_n = f_n = \frac{n\pi}{b} = k_x \tag{78}$$

This checks with Equation 76 and 77. From trigonometric identities, we have

$$\sin k_x L = (-1)^{n+1} \sin k_x a \tag{79}$$

$$\cos k_x L = (-1)^n \cos k_x a \tag{80}$$

$$\sin 2k_x L = 2\sin k_x L \cos k_x L = - 2\sin k_x a \cos k_x a \tag{81}$$

Putting the above identities in Equations 46 and 66 as $\epsilon_1 \to \epsilon_0$ yields

$$\gamma_h^{\pm} \to \pm j\omega\mu_0 \cos k_y y \sum_{n=1}^{\infty} \frac{\sin \frac{n\pi}{b} d \sin \frac{n\pi}{b} x \, e^{\mp \Gamma_n z}}{(k_y^2 - \Gamma_n^2)b} \tag{82}$$

and

$$\gamma_e^{\pm} \to - k_y \sin k_y y \sum_{n=1}^{\infty} \frac{(\frac{n\pi}{b}) \sin \frac{n\pi}{b} d \cos \frac{n\pi}{b} x \, e^{\mp \Gamma_n z}}{(k_y^2 - \Gamma_n^2) \Gamma_n b} \tag{83}$$

Since L = b in Equations 73 and 74, Equations 82 and 83 compare with the results of letting a → 0.

V. THE OPEN MICROSTRIP

The open microstrip configuration is shown in Figure 1 with $b = \infty$.

Before going to the open system, we will consider some more aspects of

the shielded microstrip.

The normal mode wave functions for the TE_x and TM_x modes of the

shielded microstrip structure are given by Equations 25 and 48, respec-

tively. These wave functions can be written in the form

$$\psi_{hn}^{\pm} = C_n \phi_{hn}(x) \cos k_y y e^{\mp \Gamma_n z} \tag{84}$$

$$\psi_{en}^{\pm} = D_n \phi_{en}(x) \sin k_y y e^{\mp \gamma_n z} \tag{85}$$

where the ϕ's contain the x dependence. ϕ_{hn} and ϕ_{en} are both solutions

of Sturm-Liouville systems (13). These systems are

$$\frac{d^2 \phi_{hn}}{dx^2} + [\Gamma_n^2 - k_y^2 + \frac{\epsilon(x)}{\epsilon_o} k_o^2]\phi_{hn} = 0 \tag{86}$$

$$\phi_{hn} = 0 \quad x = 0, b \tag{87}$$

$$\frac{d}{dx}[\frac{\epsilon_o}{\epsilon(x)} \frac{d\phi_{en}}{dx}] + \frac{\epsilon_o}{\epsilon(x)} [\frac{\epsilon(x)}{\epsilon_o} k_o^2 + \gamma_n^2 - k_y^2]\phi_{en} = 0 \tag{88}$$

$$\frac{d\phi_{en}}{dx} = 0 \quad x = 0, b \tag{89}$$

Equations 86 and 88 are both of the form

$$\frac{d}{dx}[P(x) \frac{du}{dx}] + [\lambda S(x) - Q(x)]u = 0 \tag{90}$$

where

$$Q_h = k_y^2 - \epsilon_r(x) k_o^2 \tag{91}$$

$$Q_e = k_y^2/\varepsilon_r(x) - k_o^2 \tag{92}$$

$$\varepsilon_r(x) = \varepsilon(x)/\varepsilon_o \tag{93}$$

For the open microstrip, $b = \infty$. A boundary value problem of this type is called singular and $x = b$ is called a singular point (18). Consider the limit of Q_e and Q_h as $x \to \infty$. We have

$$\lim_{x \to \infty} Q_e = \lim_{x \to \infty} Q_h = Q_o = k_y^2 - k_o^2 \tag{94}$$

The following conclusions concerning the spectrum of the boundary value problem can be made (19, 20). For $\gamma^2, \Gamma^2 < Q_o$, the TE_x and TM_x modal spectrum is discrete. The TE_x and TM_x modes form a continuous spectrum for $\gamma^2, \Gamma^2 > Q_o$. When $k_y = 0$, the above conclusions compare with known results (13).

We now consider the discrete spectrum in detail. The discrete spectrum should be proper (meets the radiation condition) (21). The radiation condition states that there can be no sources of radiation at infinity (17). This condition can be met by considering only the transverse propagation constants, $k_{x2} = r + js$, that represent waves that decay with x in the region $x > a$. Tamir and Oliner (21) have stipulated the radiation condition as

$$s = Im\ k_{x2} < 0 \tag{95}$$

In section IV, the fields for the shielded microstrip were found. Putting condition (95) into the shielded microstrip equations and letting $b \to \infty$ should result in the discrete spectrum for the open microstrip. The closed system characteristic equations are

$$f_n \cot f_n a = - t_n \cot t_n L \tag{96}$$

$$\frac{p_n}{\epsilon_1} \tan p_n a = - \frac{q_n}{\epsilon_o} \tan q_n L \tag{97}$$

Let $L = b - a \to \infty$ in Equations 96 and 97 and require that t_n and q_n meet condition (95).

$$\lim_{L \to \infty} \cot k_{x2} L = \lim_{L \to \infty} j \frac{e^{j(r+js)L} + e^{-j(r+js)L}}{e^{j(r+js)L} - e^{-j(r+js)L}} = j \tag{98}$$

$$\lim_{L \to \infty} \tan k_{x2} L = - j \tag{99}$$

Equations 96 and 97 become

$$f_n \cot f_n a = - u_n \tag{100}$$

$$\frac{p_n}{\epsilon_1} \tan p_n a = \frac{w_n}{\epsilon_o} \tag{101}$$

where $u_n = j t_n$ and $w_n = j q_n$. Equations 100 and 101 are the characteristic equations for the discrete spectrum TE_x and TM_x open microstrip modes, respectively. These equations compare exactly with the characteristic equations for the y independent TE_z and TM_z surface wave modes for the grounded dielectric slab (13). We shall call the modes in the discrete spectrum of the open microstrip configuration surface wave modes. This designation does not completely align with the usual surface wave definition because we have $k_y \neq 0$. A glance at Equations 24 and 47 shows that our TE_x and TM_x modes become also TE_z and TM_z, respectively, when $\frac{\partial}{\partial y} = 0$.

Brown (22) shows that solutions of Equations 100 and 101 exist only if t_n and q_n are pure imaginary. From condition (95), $u_n > 0$ and $w_n > 0$. Before proceeding, we need the following limits.

$$\lim_{L\to\infty} \frac{\sin t(b-\alpha)}{\sin tL} = \lim_{L\to\infty} \frac{\sinh u(b-\alpha)}{\sinh uL} = \lim_{b\to\infty} \frac{e^{u(b-\alpha)} - e^{-u(b-\alpha)}}{e^{u(b-a)} - e^{-u(b-a)}} = e^{-u(\alpha-a)}$$

(102)

Similarly,

$$\lim_{L\to\infty} \frac{\sin q(b-\alpha)}{\sin qL} = e^{-w(\alpha-a)}$$

(103)

Also,

$$\lim_{L\to\infty} \frac{L}{\sin tL} = \lim_{L\to\infty} \frac{L}{\cos qL} = 0$$

(104)

$$\lim_{L\to\infty} \frac{\sin 2tL}{\sin^2 tL} = 2j = - \lim_{L\to\infty} \frac{\sin 2qL}{\cos^2 qL}$$

(105)

$$\lim_{L\to\infty} \frac{\sin q(b-\alpha)}{\cos qL} = - je^{-w(\alpha-a)}$$

(106)

$$\lim_{L\to\infty} \frac{\cos q(b-\alpha)}{\cos qL} = e^{-u(\alpha-a)}$$

(107)

As $b \to \infty$, the results of section IV for the shielded microstrip should pass over into the solution for the open microstrip (23). The limiting process may require losses in the system (24). Putting losses in the system is equivalent to meeting the radiation condition. In letting $L \to \infty$ in the limits above, we have taken the radiation condition into account. Taking the limit in Equations 46 and 66, as $L \to \infty$, results in the following wave functions for the discrete spectrum of the open microstrip.

$$\hat{\psi}_h^{\pm} = \pm 2\omega\mu_o \cos k_y y \sum_n \frac{u_n f_n e^{\mp\Gamma_n z} e^{-u_n(d-a)}\left\{\frac{\sin f_n x}{\sin f_n a}[1-u(x-a)]+e^{-u_n(x-a)}u(x-a)\right\}}{(k_y^2-\Gamma_n^2)\left\{\frac{(-2ju_n f_n a + ju_n \sin 2f_n a)}{\sin^2 f_n a} - 2jf_n\right\}}$$

$$(108)$$

$$\hat{\psi}_e^{\pm} = -2k_y \sin k_y y \sum_n \frac{p_n w_n^2 e^{\mp\gamma_n z} e^{-w_n(d-a)}\left\{\frac{\cos p_n x}{\cos p_n a}[1-u(x-a)]+e^{-w_n(x-a)}u(x-a)\right\}}{(k_y^2-\gamma_n^2)\gamma_n\left\{\frac{\epsilon_o(2ap_n w_n + w_n \sin 2p_n a)}{\epsilon_1 \cos^2 p_n a} + 2p_n\right\}}$$

$$(109)$$

where

$$f_n^2 + k_y^2 - \Gamma_n^2 = k_1^2 = p_n^2 + k_y^2 - \gamma_n^2 \tag{110}$$

$$-u_n^2 + k_y^2 - \Gamma_n^2 = k_o^2 = -w_n^2 + k_y^2 - \gamma_n^2 \tag{111}$$

In Appendix B, Equation 108, with $k_y = 0$, is shown to compare with other known results. The symbol $\wedge$ is used to denote the discrete spectrum. The sums on n indicated in Equations 108 and 109 are both over a finite number of terms. Although there may be no terms in the expansion for $\hat{\psi}_h$, $\hat{\psi}_e$ will be found to have at least one term.

Information about the propagation properties of the surface wave modes can be gained by considering a graphical method for finding the propagation constants (13). For the TE_{xn} modes, Equations 100, 110, and 111 must be solved for f_n, u_n, and Γ_n where $n = 1, 3, \cdots$. The numbering system is chosen to correspond with the odd TE_{zn} two-dimensional surface

waves. Subtracting Equation 111 from 110 yields

$$(af)^2 + (au)^2 = a^2 \omega^2 \mu_o (\epsilon_1 - \epsilon_o) = (ak_o)^2 (\tau - 1) \tag{112}$$

where

$$\tau = \epsilon_1 / \epsilon_o \tag{113}$$

Multiplying Equation 100 by a results in

$$au = - af \cot fa \tag{114}$$

For the TM_{xn} modes, Equations 101, 110, and 111 must be solved for p_n, w_n, and γ_n where $n = 0, 2, \cdots$. The numbering system corresponds with the even TM_{zn} two-dimensional surface waves. Proceeding as above yields

$$(ap)^2 + (aw)^2 = (ak_o)^2 (\tau - 1) \tag{115}$$

$$aw = \frac{ap}{\tau} \tan pa \tag{116}$$

Equations 112, 114, 115, and 116 can be solved graphically as shown in Figure 5. In the plot, pa, fa, ua, and wa are measured on the same scales. Equations 112 and 115 are drawn as circles of radius $k_o a \sqrt{\tau - 1}$. The only valid solutions are for $u > 0$ and $w > 0$. For this reason, the plots of Equations 116 and 114 are drawn only in the first quadrant. The TM_{xn} and TE_{xn} curves could alternately be drawn along the (pa,fa) axis. However, the first two curves are sufficient to examine the theory. The straight line in Figure 5 will be discussed later.

The frequency dependence of the discrete spectrum can be clearly explained with Figure 5. The radius of the circle is proportional to frequency. Even as $\omega \to 0$, the circle intersects the TM_{xo} curve. The TM_{xo} mode always exists and at low frequencies it is the only mode in the discrete spectrum. For ω small, w_o is small and positive. If
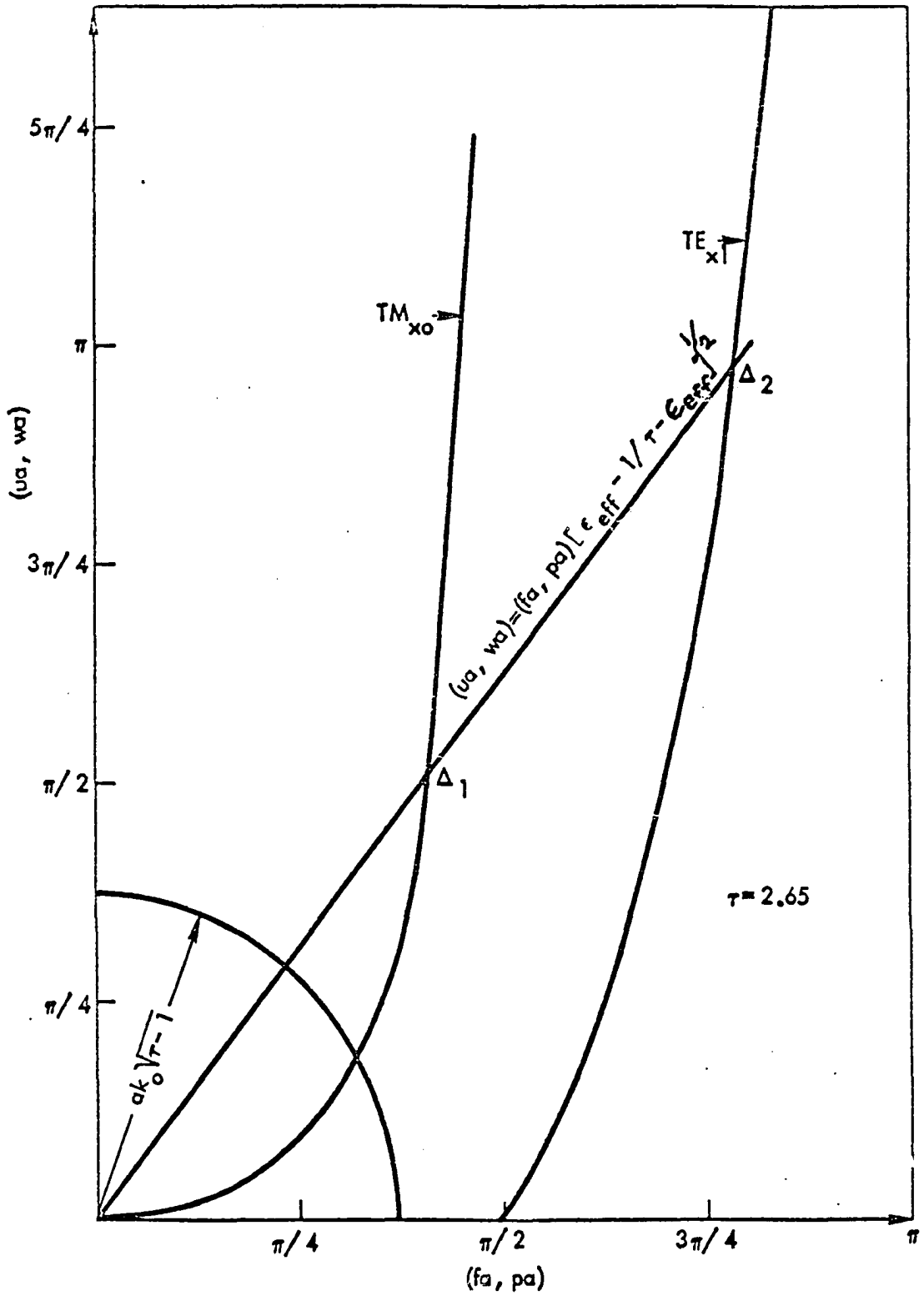
Figure 5. Graphical solution for propagation constants

$\epsilon_1 > \epsilon_0$, $k_y > k_0$ because $k_y^2/k_0^2 = \epsilon_{effective}$ where $\tau > \epsilon_{eff} > 1$. When $\tau = 2.65$, $\epsilon_{eff} \approx 2$ (8). According to Equation 111, $\gamma_0^2 > 0$ when ω is sufficiently small. As ω increases, w_0 and $k_y^2 - k_0^2 = k_0^2 (\epsilon_{eff} - 1)$ increase. For large ω, w_0^2 goes as $k_0^2(\tau-1)$ which can be expected to be at least $1.2 \, k_0^2 \, (\epsilon_{eff} - 1)$ (7). At some ω, γ_0^2 goes negative. We can conclude that although the TM_{xo} mode always exists it does not propagate in the z direction until ω becomes sufficiently large. The frequency at which the TE_{x1} mode comes into existence is

$$f_c = \frac{\pi/2 \; v_0}{2\pi a \sqrt{\tau-1}} = \frac{v_0}{4a\sqrt{\tau-1}} = \frac{\omega_c}{2\pi} \qquad (117)$$

where

$$v_0 = \frac{1}{\sqrt{\epsilon_0 \mu_0}} \qquad (118)$$

Although the TE_{x1} mode exists at $\omega = \omega_c$, it does not propagate in the z direction until ω becomes sufficiently greater than ω_c.

The frequencies at which the TM_{xn} and TE_{xn} microstrip modes come into existence are the cutoff frequencies of the TM_{zn} and TE_{zn}, two-dimensional, grounded dielectric slab modes. The two-dimensional surface waves always propagate in the z direction when $\omega > \omega_c$. However, it was found above that this isn't the case for the open microstrip surface waves.

The frequency at which the surface wave modes come into existence has been found graphically. A graphical method can also be used to determine the frequency at which the surface wave modes begin to propagate. To develop the method, put Γ_n and γ_n equal to zero in Equations 111.

This results in

$$(au_n)^2 = a^2(k_y^2 - k_o^2) = (ak_o)^2(\varepsilon_{eff} - 1) = (aw_n)^2 \tag{119}$$

Substituting Equations 119 into Equations 112 and 115 yields

$$au_n = (\frac{\varepsilon_{eff} - 1}{\tau - \varepsilon_{eff}})^{\frac{1}{2}} a \ f_n \tag{120}$$

$$aw_n = (\frac{\varepsilon_{eff} - 1}{\tau - \varepsilon_{eff}})^{\frac{1}{2}} a \ p_n \tag{121}$$

A line representing both Equation 120 and Equation 121 is drawn in Figure 5. This can be called the cutoff line. If the circle intersects the TM_{xo} curve or the TE_{x1} curve above the cutoff line, the TM_{xo} mode or the TE_{x1} mode propagates in the z direction. When the circle passed between point Δ_1 and point Δ_2 only the TM_{xo} mode propagates. In Figure 5, the cutoff line is drawn for $\tau = 2.65$. We have assumed that ε_{eff} is independent of frequency. This assumption is reasonable for $\tau = 2.65$ (8). However, ε_{eff} actually increases toward τ with frequency (7). This means that as the radius of the circle in Figure 5 increases the slope of the cutoff line increases.

VI. NUMERICAL RESULTS

A. The Shielded Microstrip

In section V, $\phi_{en}(x)$ and $\phi_{hn}(x)$ were discussed as solutions of Sturm-Liouville problems. The eigenvalues of the associated Sturm-Liouville problems are γ_n^2 and Γ_n^2. A variational expression for γ_n^2 and Γ_n^2 is developed by Collin (13). The variational expressions are

$$\gamma_n^2 = \frac{\int_0^b \frac{1}{\epsilon_r(x)}\{(\frac{d\phi_{en}}{dx})^2 - [\epsilon_r(x)k_o^2 - k_y^2]\phi_{en}^2\}dx}{\int_0^b \frac{1}{\epsilon_r(x)} \phi_{en}^2 dx} \tag{122}$$

and

$$\Gamma_n^2 = \frac{\int_0^b \{(\frac{d\phi_{hn}}{dx})^2 - [\epsilon_r(x)k_o^2 - k_y^2]\phi_{hn}^2\}dx}{\int_0^b \phi_{hn}^2 \, dx} \tag{123}$$

The eigenvalues form the following monotonically increasing sequences.

$$\gamma_o^2 < \gamma_1^2 < \gamma_2^2 \cdots < \gamma_n^2 \tag{124}$$

$$\Gamma_1^2 < \Gamma_2^2 < \Gamma_3^2 \cdots < \Gamma_n^2 \tag{125}$$

ϕ_{en} and ϕ_{hn} are unknown because the propagation constants t_n, f_n, q_n and p_n are unknown. A suitable set of functions to use for the extremization of Equations 122 and 123 are the empty guide eigenfunctions (13). The empty guide eigenfunctions are

$$g_{en} = (\frac{2}{b})^{\frac{1}{2}} \cos \frac{n\pi}{b} x \qquad n = 1,2,3 \cdots \tag{126}$$

$$g_{eo} = (\frac{1}{b})^{\frac{1}{2}} \tag{127}$$

$$g_{hn} = (\frac{2}{b})^{\frac{1}{2}} \sin \frac{n\pi}{b} x \qquad\qquad n = 1,2,3 \cdots \qquad\qquad (128)$$

Substitution of g_{en} and g_{hn} for ϕ_{en} and ϕ_{hn} in Equations 122 and 123 yields an upper bound for the true eigenvalues γ_n^2 and Γ_n^2. Equations 122 and 123 can be expected to give good approximations for γ_o^2 and Γ_1^2, especially when ϵ_1 does not differ greatly from ϵ_o (14). This method can also be used to find approximations for the higher order eigenvalues. However, the accuracy of the approximation is questionable (25). The results of putting Equations 126, 127, and 128 into Equations 122 and 123 are

$$\gamma_o^2 \approx \frac{- k_o^2}{\frac{1}{b}(L + \frac{\epsilon_o}{\epsilon_1} a)} + k_y^2 \qquad\qquad (129)$$

$$\gamma_n^2 \approx k_y^2 + \frac{(\frac{n\pi}{b})^2[1 - (1 - \frac{\epsilon_o}{\epsilon_1})(\frac{a}{b} - \frac{\sin \frac{2n\pi}{b} a}{2n\pi})] - k_o^2}{[1 - (1 - \frac{\epsilon_o}{\epsilon_1})(\frac{a}{b} + \frac{\sin \frac{2n\pi}{b} a}{2n\pi})]} \qquad\qquad (130)$$

$n = 1,2,3, \cdots$

$$\Gamma_n^2 \approx k_y^2 + (\frac{n\pi}{b})^2 - k_o^2[1 - (1 - \frac{\epsilon_1}{\epsilon_o})(\frac{a}{b} - \frac{\sin \frac{2n\pi}{b} a}{2n\pi})] \qquad\qquad (131)$$

$n = 1,2,3 \cdots$

As a numerical example consider the shielded microstrip with

$d = a = .127 \times 10^{-2}$ m

$b = 10$ a

$\epsilon_1/\epsilon_o = \tau = 4.2$

$$f = 2 \text{ GHz}$$

Using the results of Zysman and Varon (8), we have $k_y \approx 1.7 \, k_o$. The results of using Equations 129, 130 and 131 are $\gamma_o \approx 56.1$, $\Gamma_1 \approx 253$, and $\gamma_1 \approx 273$.

Consider another example with everything the same as above except with $\tau = 2.65$. For this case, $k_y \approx 1.42 \, k_o$. The propagation constants are found to be $\gamma_o \approx 40.5$, $\Gamma_1 \approx 258$, $\gamma_1 \approx 266$ and $\Gamma_2 \approx 497$. Since ϵ_1 does not differ greatly from ϵ_o, it is expected that Equations 130 and 131 give reasonably accurate results for γ_1 and Γ_2. From Equations 27, 28, 49 and 50, it is found that $q_o \approx - j10.95$, $p_o \approx 52.6$, $q_1 \approx 262$, $p_1 \approx 268$, $t_1 \approx 254$, and $f_1 \approx 260$. Letting $a = d$ and putting Equations 46 and 66 into Equations 24 and 47, respectively, results in the following fields.

$$E_{yeo}(a, \, 0, \, z) \approx 1.36 \, e^{-40.5z} \tag{132}$$

$$E_{yh1}(a, \, 0, \, z) \approx - j \, 310e^{-258z} \tag{133}$$

$$E_{ye1}(a, \, 0, \, z) \approx j \, 403e^{-266z} \tag{134}$$

Let

$$\theta = \frac{\left| E_{yh1}(a,0,z) + E_{ye1}(a,0,z) \right|}{\left| E_{yh1}(a,0,0) + E_{ye1}(a,0,0) \right|} \tag{135}$$

In Figure 6, θ versus z/a is plotted. The higher order modal fields are expected to decay, with z, at least as fast as the TE_{x2} mode. Since $\Gamma_2 \approx 467$ and γ_1, $\Gamma_1 \approx .52 \, \Gamma_2$, the plot of Figure 6 should be a reasonable approximation for the total microstrip field decay when $z/a > 3$.
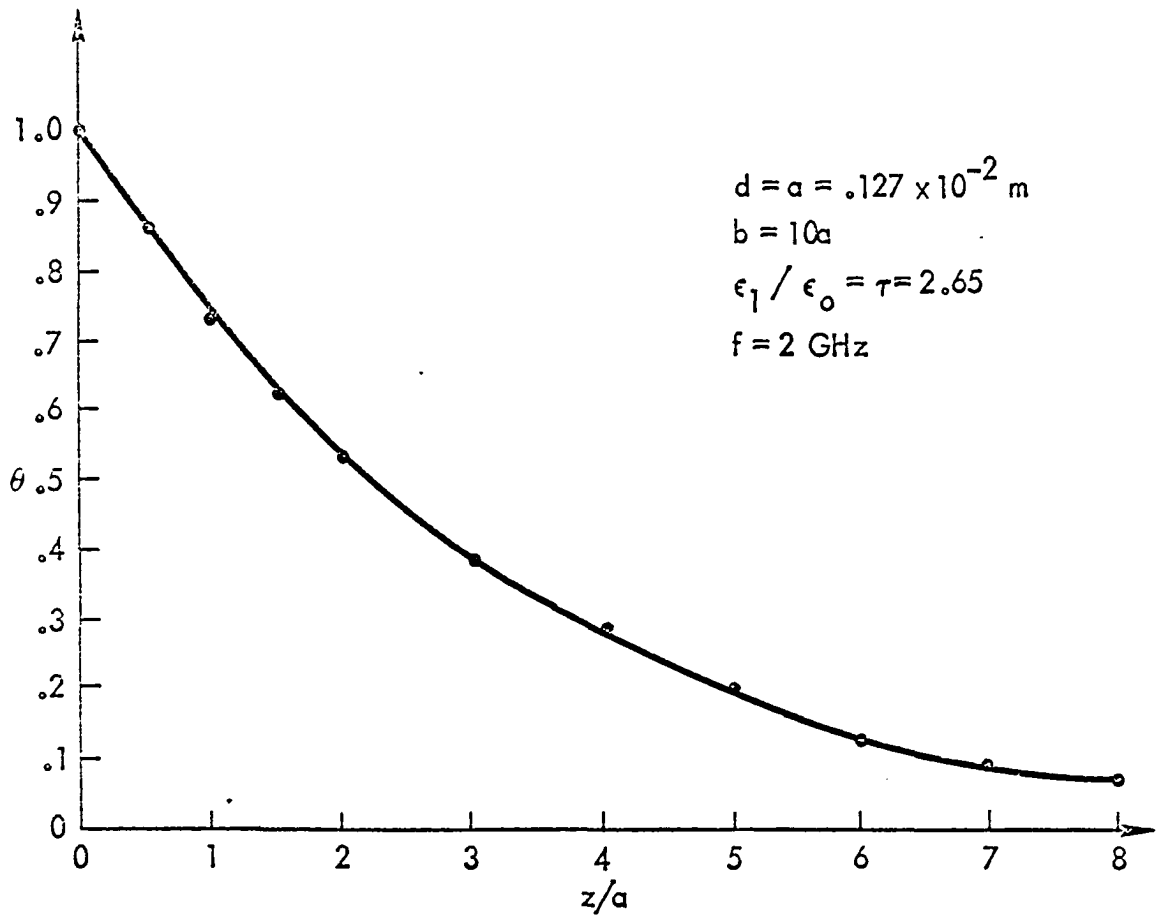
$$d = a = .127 \times 10^{-2} \, m$$
$$b = 10a$$
$$\epsilon_1 / \epsilon_o = \tau = 2.65$$
$$f = 2 \, GHz$$

Figure 6. Normalized E_y versus distance from the conductor

B. The Open Microstrip

Consider an open microstrip transmission line with $f = 10$ GHz, $\tau = \epsilon_1/\epsilon_o = 2.65$, and $a = .127 \times 10^{-2}$ m. For this line, $k_y \approx \sqrt{2} \, k_o$ (8). The graphical method discussed in section V can be used to determine the surface waves associated with the microstrip and the propagation constants. We have

$$a \, k_o \sqrt{\tau - 1} = a \, \frac{\omega}{v_o} \sqrt{\tau - 1} = .342$$

Using Figure 5, it is seen that the discrete spectrum consists only of the TM_{xo} mode. Also, we find that $w_o \approx 41.3$. γ_o can be found by using Equation 111. The result is

$$\gamma_o = \sqrt{- w_o^2 + k_y^2 - k_o^2} = \sqrt{- w_o^2 + k_o^2} = 205.$$

The TM_{xo} mode does not propagate in the z direction at $f = 10$ GHz. By trial and error, it was found that the frequency where propagation in the z direction begins for the TM_{xo} mode is about 61.5 GH_z. This agrees with the theory of section V.

VII. SUMMARY AND CONCLUSION

The electromagnetic fields of the shielded microstrip transmission line have been found in terms of the normal modes of the dielectric slab waveguide. A method of summing the modes propagating transverse to the conductor is used to find the field representation. To check the solution, two separate limiting processes are shown to reduce the shielded microstrip transmission line to the stripline configuration.

The discrete modal spectrum of the open microstrip transmission line is studied in detail. These modes are found to be a three-dimensional generalization of well-known two-dimensional surface waves. It is shown that the microstrip surface waves can exist without propagating away from the conductor. A graphical method is developed to determine the existence and the propagation properties of the surface wave modes associated with the microstrip line. It is found that predictions based on a two-dimensional surface wave analysis may be erroneous. A TM mode is found to exist on the microstrip at all frequencies.

VIII. LITERATURE CITED

1. Wheeler, H. A. Transmission-line properties of parallel strips separated by a dielectric sheet. IEEE Trans. Microwave Theory and Techniques MTT-13: 172-185. March 1965.

2. Hill, Y. M., N. O. Reckord, and D. R. Winner. A general method for obtaining impedance and coupling characteristics of practical microstrip and triplate transmission line configurations. I.B.M. Journal of Research and Development 13: 314-322. May 1969.

3. Green, H. F. The numerical solution of some important transmission-line problems. IEEE Trans. Microwave Theory and Techniques MTT-13: 676-692. September 1965.

4. Yamashita, E. and R. Mittra. Variational method for the analysis of microstrip lines. IEEE Trans. Microwave Theory and Techniques MTT-16: 251-256. April 1968.

5. Weeks, W. L. Electromagnetic theory for engineering applications. New York, New York, John Wiley and Sons, Inc. 1964.

6. Wu, T. T. Theory of the microstrip. Journal of Applied Physics 28: 299-302. March 1957.

7. Denlinger, E. J. A dynamic TE-TM mode solution for the microstrip. 1969 IEEE G-MTT International Microwave Symposium, Dallas, Texas, May 1969. Lexington, Mass., Lincoln Laboratory. 1969.

8. Zysman, G. I. and D. Varon. Wave propagation in microstrip transmission lines. IEEE G-MTT International Symposium Digest 1969: 3-9. May 1969.

9. Hartwig, C. P., D. Masse and R. A. Pucel. Frequency dependent behaviour of microstrip. IEEE G-MTT International Symposium Digest 1968: 110-119. 1968.

10. Pucel, R. A., D. J. Masse, and C. P. Hartwig. Losses in microstrip. IEEE Trans. Microwave Theory and Techniques MTT-16: 342-350. June 1968.

11. Bryant, T. G. and J. A. Weiss. Parameters of microstrip transmission lines and of coupled pairs of microstrip lines. IEEE Trans. Microwave Theory and Techniques MTT-16: 1021-1027. December 1968.

12. Weeks, W. L. Antenna engineering. New York, New York, McGraw-Hill Book Company. 1968.

13. Collin, R. E. Field theory of guided waves. New York, New York, McGraw-Hill Book Company. 1960.

14. Harrington, R. F. Time-harmonic electromagnetic fields. New York, New York, McGraw-Hill Book Company. 1961.

15. Morse, P. M. and H. Feshbach. Methods of theoretical physics. Parts I and II. New York, New York, McGraw-Hill Book Company. 1953.

16. Kraut, E. A. Fundamentals of mathematical physics. New York, New York, McGraw-Hill Book Company. 1967.

17. Sommerfeld, A. Partial differential equations in physics. New York, New York, Academic Press Incorporated. 1964.

18. Stakgold, I. Boundary value problems of mathematical physics. Volume I. New York, New York, Macmillan Company. 1968.

19. Birkhoff, G. and G. Rota. Ordinary differential equations. Second edition. Waltham, Massachusetts, Blaisdell Publishing Company. 1969.

20. Titchmarch, E. C. Eigenfunction expansions. Part I. Second edition. Fairlawn, New Jersey, Oxford University Press. 1962.

21. Tamir, T. and A. A. Oliner. Guided complex waves. IEE Proceedings 110, Part 1: 310-324. February 1963.

22. Brown, J. The type of wave which may exist near a guiding surface. IEE Proceedings 100, Part 3: 363-364. November 1953.

23. Mittra, R., D. S. Kayala, and G. F. Van Blaricum, Jr. Solution of an open region problem as a limiting case of a closed region problem. Applied Scientific Research 16: 169-177. 1966.

24. Bates, C. P. A technique for solving certain Wiener-Hopf type boundary value problems. Unpublished Ph.D. thesis. Urbana, Ill., Library, University of Illinois. 1966.

25. Morse, P. M. and K. U. Ingard. Theoretical acoustics. New York, New York, McGraw-Hill Book Company, Inc. 1968.

IX. ACKNOWLEDGMENTS

X. APPENDIX A

We want to evaluate C_n of Equation 25. From Equation 39, C_n is chosen so that

$$\iint\limits_{S} \vec{e}_{hn} \times \vec{h}_{hn} \cdot \vec{a}_z \, da = 1 \tag{136}$$

where $\vec{e}_{hn}$ and $\vec{h}_{hn}$ are given by Equations 37 and 38, respectively. Substituting into Equation 136 yields

$$\int_{-y_1}^{y_1} \int_{0}^{b} \frac{C_n^2 \Gamma_n (\Gamma_n^2 - k_y^2) \cos^2 k_y y}{j \omega \mu_o} \left\{ \frac{\sin^2 t_n L}{\sin^2 f_n a} \sin^2 f_n x [1 - u(x-a)] \right.$$
$$\left. + \sin^2 t_n (b-x) u(x-a) \right\} dx \, dy = 1 \tag{137}$$

where $y_1 = \pi/k_y$. Performing the integration, we have

$$1 \approx \frac{\pi (\Gamma_n^2 - k_y^2) \Gamma_n C_n^2}{j k_y \omega \mu_o} \left\{ \frac{\sin^2 t_n L}{\sin^2 f_n a} \left(\frac{a}{2} - \frac{\sin 2 f_n a}{4 f_n} \right) + \frac{L}{2} - \frac{\sin 2 t_n L}{4 t_n} \right\} \tag{138}$$

The result of solving for C_n^2 is

$$C_n^2 = \frac{-4 j \omega \mu_o k_y t_n f_n}{\Gamma_n (k_y^2 - \Gamma_n^2) \pi \left\{ \dfrac{\sin^2 t_n L}{\sin^2 f_n a} (2 t_n f_n a - t_n \sin 2 f_n a) + 2 t_n f_n L - f_n \sin 2 t_n L \right\}} \tag{139}$$

D_n of Equation 48 must also be evaluated. From Equation 60, D_n is chosen so that

$$\iint\limits_{S} \vec{e}_{en} \times \vec{h}_{en} \cdot \vec{a}_z \, da = 1 \tag{140}$$

where $\vec{e}_{en}$ and $\vec{h}_{en}$ are given by Equations 58 and 59. Substituting into Equation 140 yields

$$-\int_{-y_1}^{y_1}\int_0^b \frac{(k_y^2-\gamma_n^2)\gamma_n D_n^2 \sin^2 k_y y}{j\omega\varepsilon(x)}\{\frac{\cos^2 q_n L}{\cos^2 p_n a}\cos^2 p_n x[1-u(x-a)]$$

$$+\cos^2 q_n(b-x)u(x-a)\}dxdy = 1 \qquad (141)$$

Integrating, we have

$$1 = \frac{j(k_y^2-\gamma_n^2)\gamma_n D_n^2 \pi}{\omega k_y}\{\frac{\cos^2 q_n L}{\varepsilon_1 \cos^2 p_n a}(\frac{a}{2}+\frac{\sin 2p_n a}{4p_n}) + \frac{L}{2\varepsilon_o} + \frac{\sin 2q_n L}{4q_n \varepsilon_o}\} \qquad (142)$$

Solving for D_n^2 yields

$$D_n^2 = \frac{-4j\omega k_y p_n q_n \varepsilon_o}{(k_y^2-\gamma_n^2)\gamma_n \pi\{\frac{\varepsilon_o \cos^2 q_n L}{\varepsilon_1 \cos^2 p_n a}(2p_n q_n a + q_n \sin 2p_n a) + 2p_n q_n L + p_n \sin 2q_n L\}}$$

$$(143)$$

XI. APPENDIX B

The purpose of this appendix is to compare $\hat{\psi}_h^+$ of Equation 108 with other known results. For the case when $k_y = 0$, Collin (13) gives $\hat{E}_{hy}^+$ for $x \geq a$ as

$$\hat{E}_{hy}^+ = \frac{\omega\mu_0}{2} \sum_n \text{Residues } \frac{N(\Gamma)}{M(\Gamma)} \tag{144}$$

where

$$N(\Gamma) = (u - f\cot fa)e^{-u(x+d-2a)}e^{-\Gamma z} \tag{145}$$

$$M(\Gamma) = -ju(u + f\cot fa) \tag{146}$$

$$-ju = (\Gamma^2 + k_0^2)^{\frac{1}{2}} \tag{147}$$

$$f = (\Gamma^2 + k^2)^{\frac{1}{2}} \tag{148}$$

The zeros of $M(\Gamma)$ are of first order and lie on the imaginary axis of the Γ-plane between jk_0 and jk (13). From Equation 146, it is seen that the zeros of $M(\Gamma)$ are the solutions of Equation 100. The following formula will be used to find the residues (16).

$$\text{Residue } [\frac{N(\Gamma)}{M(\Gamma)}, \Gamma = \Gamma_n] = \lim_{\Gamma \to \Gamma_n} \frac{N(\Gamma)}{\frac{dM}{d\Gamma}} \tag{149}$$

We have,

$$\frac{df}{d\Gamma} = \frac{\Gamma}{f} \tag{150}$$

$$\frac{d(-ju)}{d\Gamma} = \frac{j\Gamma}{u} \tag{151}$$

$$\frac{dM}{d\Gamma} = \Gamma\{2j+juacsc^2 fa - j\,\frac{u}{f}\,cotfa + j\,\frac{f}{u}\,cotfa\} \tag{152}$$

Using Equations 100 and 149 yields

$$\text{Residue}\,[\frac{N(\Gamma)}{M(\Gamma)},\ \Gamma = \Gamma_n] = \frac{-\,4u_n f_n e^{-u_n(x-a)}\,e^{-u_n(d-a)}\,e^{-\Gamma_n z}}{j\,\Gamma_n\{\dfrac{u_n sin2f_n a\,-\,2u_n f_n a}{sin^2 f_n a} - 2f_n\}} \tag{153}$$

The result of substituting Equation 153 into Equation 144 is

$$\hat{E}^+_{hy} = 2j\omega\mu_o \sum_n \frac{u_n f_n e^{-u_n(x-a)}\,e^{-u_n(d-a)}\,e^{-\Gamma_n z}}{\Gamma_n\{\dfrac{u_n sin2f_n a - 2u_n f_n a}{sin^2 f_n a} - 2f_n\}} \tag{154}$$

This checks with the solution in section V when $k_y = 0$ and $x \geq a$.